Journal of Applied Electrochemistry **32**: 1279–1285, 2002.

Influence of preparation process of MEA with mesocarbon microbeads supported Pt–Ru catalysts on methanol electrooxidation

Y-C. LIU, X-P. QIU*, Y-Q. HUANG, W-T. ZHU and G-S. WU
Department of Chemistry, Tsinghua University, Beijing 100084, Peoples' Republic of China
*(*author for correspondence, e-mail: qiuxp@mail.tsinghua.edu.cn)*

Received 7 February 2002; accepted in revised form 30 July 2002

Key words: MCMB, methanol electrooxidation, Pt–Ru catalyst

Abstract

The effects of mesocarbon microbeads support for platinum–ruthenium (Pt–Ru) catalysts on anode performance of the direct methanol fuel cell (DMFC) were investigated. Polarization characteristics of the anode electrode were low due to the fast rate of mass transport in the electrode. The effects of the Nafion® content in the catalyst, the MEA hot press condition, the cell operation temperature and methanol concentration on the polarization curves of the anode were also investigated.

1. Introduction

The direct methanol fuel cell (DMFC) is one of the most desirable fuel cells for small-scale power units [1–3]. To date, Pt–Ru alloy catalysts are still considered as the most active catalysts to improve the effective polarization characteristics of methanol electrooxidation for DMFCs [4–10]. These catalysts are generally dispersed in small particles on conductive supports such as carbon blacks with a high specific surface area to obtain the optimum catalyst [11–17]. In order to improve the reaction rate in the cell, mass transport in the anode should also be considered. To minimize the transport resistances in the electrochemical reaction, appropriate pore-forming additives [18,19] were introduced into the catalyst layer to increase the pore volume. In this work, mesocarbon microbeads (MCMB) was used as catalyst support. Mesocarbon microbeads derived from petroleum residua is a kind of 'hard' carbon with 1–40 μm in diameter and low specific surface area. By using MCMB as support, pores and channels in the electrocatalytic electrode remain open and favor mass transport during electrocatalytic reaction.

2. Experimental details

2.1. *Preparation and characterization of supported Pt–Ru catalysts*

MCMBs (Shanshan Inc., Shanghai) were boiled in 2 M KOH solution for 1 h before the supported catalyst preparation. The supported catalysts were prepared by liquid-phase reduction of chloroplatinic acid and ruthenium chloride with sodium hyposulfite. MCMB (3.7 g) was suspended in 200 ml of water at 80 °C. An aqueous solution (50 ml) containing 1 g chloroplatinic acid and an appropriate amount of ruthenium chloride solution (Pt:Ru molar ratio equal to 3:1) were added slowly to the MCMB suspension to achieve complete impregnation (lasting over 1 h). Then, 50 ml of 0.5 M $Na_2S_2O_4$ was added drop by drop. The resultant mixture was heated at 80 °C for 3 h to allow complete reduction of Pt and precipitation of metallic oxides. Subsequently, the mixture was filtered and washed copiously with hot distilled water to remove chloride ions. The catalyst was dried in air at 80 °C for 5 h and was heat-treated at 300 °C for 1 h.

Surface morphologies of the catalysts were examined by a thermal field emission scanning electron microscope (SEM LEO1530). X-ray diffraction (XRD: Rigaku X-ray diffractometer using a Cu target) was employed in order to study the crystal structure of the catalysts.

2.2. *Preparation and characterization of electrode*

The diffusion electrodes prepared for the investigation of the electrochemical oxidation methanol are presented in Table 1. First, the Pt–Ru/MCMB catalyst was suspended in Millipore conductivity water and agitated in an ultrasonic bath for 30 min. Subsequently, the slurry was mixed with perfluorosulfonic acid solution (5 wt%, Nafion®, Du Pont) and glycol and acetylene black (10 wt%) under ultrasonic agitation for 1 h. The amount of perfluorosulfonic acid solution was selected

Table 1. Anode parameters with all Pt loadings at 0.3 mg cm^{-2}

Anode	Nafion® content /wt%	Pressure of hot-press /MPa
1	5	7.5
2	10	7.5
3	20	7.5
4	10	5
5	10	10

to control the content of Nafion® (dry) in the catalyst. In this manner, catalyst ink was obtained which was stretched and spread on a carbon paper (Toray). All the Pt loading in the electrodes were 0.3 mg cm^{-2}. The cathode was prepared by the same method as the anode, except that acetylene black was not added. The catalyst loading in the cathode was 0.5 mg cm^{-2} Pt/C (20 wt% Pt, E-Tek Inc.). The MEA was finally obtained by hot-pressing the anode and cathode on either side of a pretreated Nafion-112™ membrane under a selected pressure at 130 °C for 3 min. The MEA so formed was typically of thickness about 1 mm. Anodes 1 to 3 contained various amounts of Nafion in the catalysts at the same hot press condition. Anodes 2, 4 and 5 contained the same amounts of Nafion but were hot pressed at different pressures.

The structure of the cell for the electrochemical measurements is shown in Figure 1. The MEA was sandwiched between two blocks of graphite into which gas/liquid flow channels were engraved. The ridges between the channels provided electrical contact to the carbon electrodes, and the total geometrical area of the cell was 3 cm^2. Electrical heaters were mounted at the rear of the graphite blocks to control the cell temperature, which was monitored by thermocouples buried in the blocks. A saturated calomel reference electrode (SCE) port was machined into the anode block (Figure 1). Current–voltage (I/V) curves were obtained using a Solartron potentiostat (Solartron 1287, Solartron Instruments), which was interfaced to a PC through National Instruments IEEE-488 GPIB card. It should be noted that the electrode polarization curves reported in this paper were not iR corrected.

3. Results and discussion

The X-Ray diffraction pattern of MCMBs supported catalyst is shown in Figure 2. The peak near $2\theta = 25°$ in the pattern corresponds to the diffraction of mesocarbon microbeads. Platinum peaks are observed at 2θ values of about 39.7°, 46.2°, 67.6° and 81.3°, corresponding to platinum (1 1 1), (2 0 0), (2 2 0) and (3 1 1), respectively. No evidence of peaks related to tetragonal RuO_2 and hexagonal close-packed Ru phases was found in the Figure 2, which indicates the presence of a Pt–Ru alloy in the catalyst. The result agrees with that of other researchers [20]. The crystal size of the supported catalysts, calculated from XRD peak widths [21], is 13.1 nm.

Figure 3 shows SEM photographs of MCMB supported catalyst. The particle size of MCMBs is about

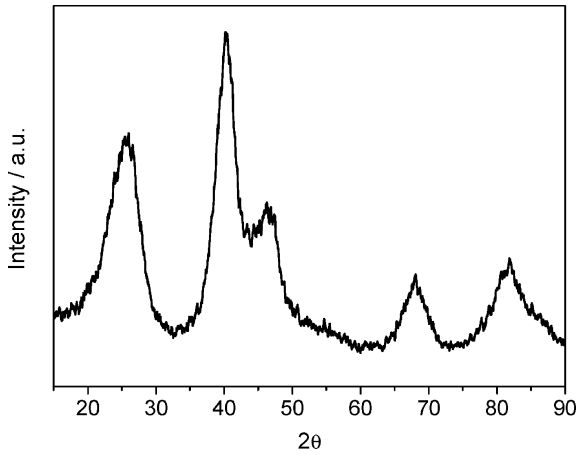

Fig. 2. XRD diffraction pattern of Pt–Ru/MCMB.

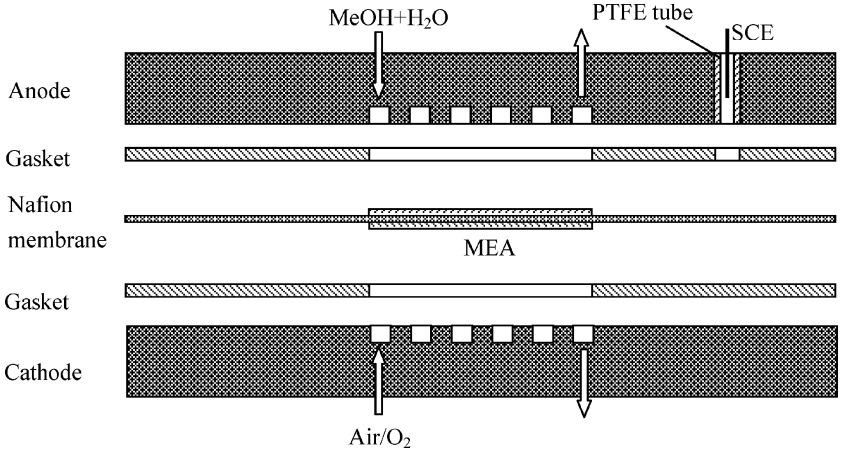

Fig. 1. Schematic diagram of the direct methanol fuel cell.

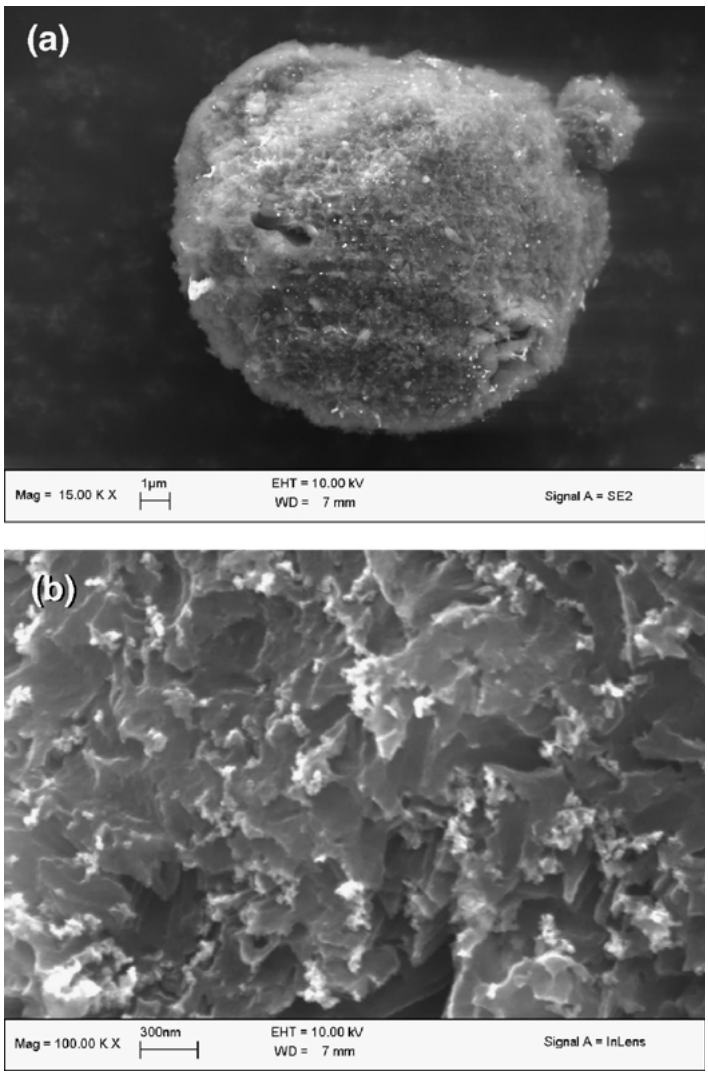

Fig. 3. SEM photograph of Pt–Ru/MCMB.

10 μm. Due to treatment in base solution, the surface of the spherules appears feathery. Many nodular lumps and pores can be observed on the surface. The surface roughness increases the specific surface of the spherules, which is helpful for the adsorption of platinum and ruthenium.

Figure 3(b) shows the morphology of noble metals adsorbed on the surface of the mesocarbon microbeads. Most of the noble metal particles are spread uniformly over the lumps on the surface. The size of the noble metal particles determined by SEM is about 10 nm, which is very close to the value calculated by the Scherrer formula as mentioned above. In Figure 3(b), agglomerates of Pt–Ru catalysts can also be observed. The size of the agglomerates is about 100 nm. Here, the Pt–Ru particle size is larger than that of catalyst prepared with carbon black with high surface area. For example, the Pt size of the supported catalyst Pt/Vulcan XC-72R is about 3.0 nm [13]. Watanabe and Uchida et al. [13, 22, 23] had demonstrated that the size of catalyst particles adsorbed onto a support surface increased with decrease in specific surface area of the carbon support. The specific surface area of MCMBs being treated in base solution was only 1.3 $m^2\ g^{-1}$, which is two orders of magnitude lower than that of carbon black (e.g., Vulcan XC-72R 254 $m^2\ g^{-1}$ [13]). This may be one of the reasons that the noble metal particle size was larger than that with the support of active carbon black.

Figure 4 shows a comparison of anode polarization curves of Pt–Ru/C (E-TEK) and Pt–Ru/MCMB (anode 2) electrodes; the electrode potential was referenced to SCE. The two electrodes were prepared and measured by the same method except that some acetylene black was added to the slurry when preparing the Pt–Ru/MCMB electrode. The Pt loading was about 0.3 mg cm^{-2} in each electrode.

The polarization curves can be roughly characterized by two regions. At low current densities, a sudden increase of about $0.2 \sim 0.3$ V of anode potential is recorded when a small current is allowed to pass through the anode, which corresponds to charge-transfer resistance at the electrode–electrolyte interface (activation control). A second region at intermediate-high

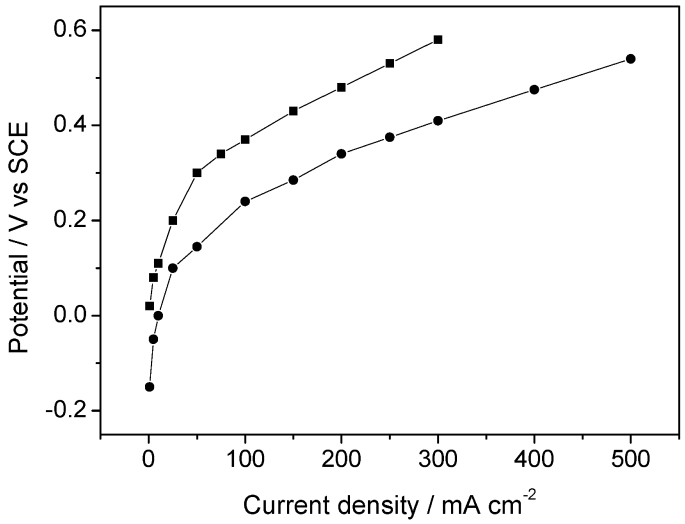

Fig. 4. Comparison of anode polarization performance against current density with Pt–Ru/C (E-TEK) and Pt–Ru/MCMB (anode 2) electrodes. Methanol concentration 1.0 M; cell temperature 90 °C; Pt loading 0.3 mg cm^{-2}. Key: (■) Pt–Ru/C. (●) Pt–Ru/MCMBs.

current density, characterized by linear variation of potential against current is mainly affected by intrinsic ohmic resistance.

The electrode with Pt–Ru/MCMB shows lower polarization performance than that of Pt–Ru/C (E-TEK). The overpotential of Pt–Ru/MCMB is 0.41 V vs SCE at 300 mA cm^{-2} at 90 °C, which is 0.17 V lower than that of Pt–Ru/C. It was reported that the overpotentials of supported Pt–Ru catalysts with various carbon black as supports ranged from $355 \sim 500$ mV vs NHE at 60 mA cm^{-2} at 60 °C with Pt loading about 2 mg cm^{-2} [13]. The overpotential of Pt–Ru/MCMB catalyst is about 0.16 V vs SCE at 60 mA cm^{-2} at 90 °C with Pt loading only 0.3 mg cm^{-2}. When the current density increases to 500 mA cm^{-2}, the overpotential is 0.54 V vs SCE. This indicates that mesocarbon microbead supported Pt–Ru catalyst exhibit a high catalytic activity for methanol electrochemical oxidation at low Pt loadings. It can be concluded that, although mesocarbon microbeads are micrometre-sized particles with low specific surface area, they are excellent candidates for use as support of Pt–Ru catalyst for methanol oxidation.

It should be noted that the Pt–Ru/MCMB catalyst was prepared using hyposulfate solution as reducer, which inevitably produced sulfur on the electrocatalyst surface. The sulfur impedes methanol electrooxidation, so the removal of sulfur would increase the catalyst performance.

For preparation of MEAs with high methanol electrochemical oxidation rate, the content of ionomer in the catalyst layer is very important. With MCMB as support, the optimum ionomer content in the catalyst layer may be different from that with active carbon black as support. Figure 5 shows the effect of Nafion® content in an electrode on anode polarization characterization for a Pt–Ru/MCMB. Anode 2 (Nafion® content: 10 wt%) shows the lowest polarization among the three samples at any cell temperature. When comparing anode 3 (Nafion® content: 20 wt%) and anode 1 (Nafion® content: 5 wt%), the polarization of anode 1 is lower at low temperature (60 °C), but higher at high temperature (90 °C). The effects of ionomer content in the catalyst layer on the performance of DMFC have been discussed by other authors [24–26]. Not only does the inclusion of Nafion® in the catalyst layer provide structural integrity, it has also been shown to be essential for sufficient ionic conductivity within the electrode structure. The specific protonic conductivity of a catalyst layer prepared with recast Nafion® is proportional to the volume fraction of Nafion® in the catalyst layer [24]. The increase in overpotential at the highest Nafion® content in the catalyst layer is due to mass transport resistance with an increase in thickness of ionomer on the Pt particles.

Figure 6 shows the dependence of the polarization curves on the pressure of the hot press during MEA preparation, the concentration of methanol feed into anode was 1 M. When pressure increased from 5.0 MPa (anode 4) to 7.5 MPa (anode 2), the anode overpotential decreased; but when the pressure increased to 10.0 MPa (anode 5), the anode overpotential increased. The hot press process ensures compact contact between the electrodes and the membrane. Loose contact increases contact resistance, but over-compaction may block the pores and channels in the catalytic layer and cause increased mass transport resistance. Therefore, an optimization of the hot press pressure may improve cell performance.

From Figures 5 and 6, it can be seen that anode 2 with appropriate Nafion® content (10 wt%) and hot pressure condition (7.5 MPa) shows the best performance compared to the other four samples.

Figure 7 shows the temperature dependence of the polarization curves of anode 2 with various concentra-

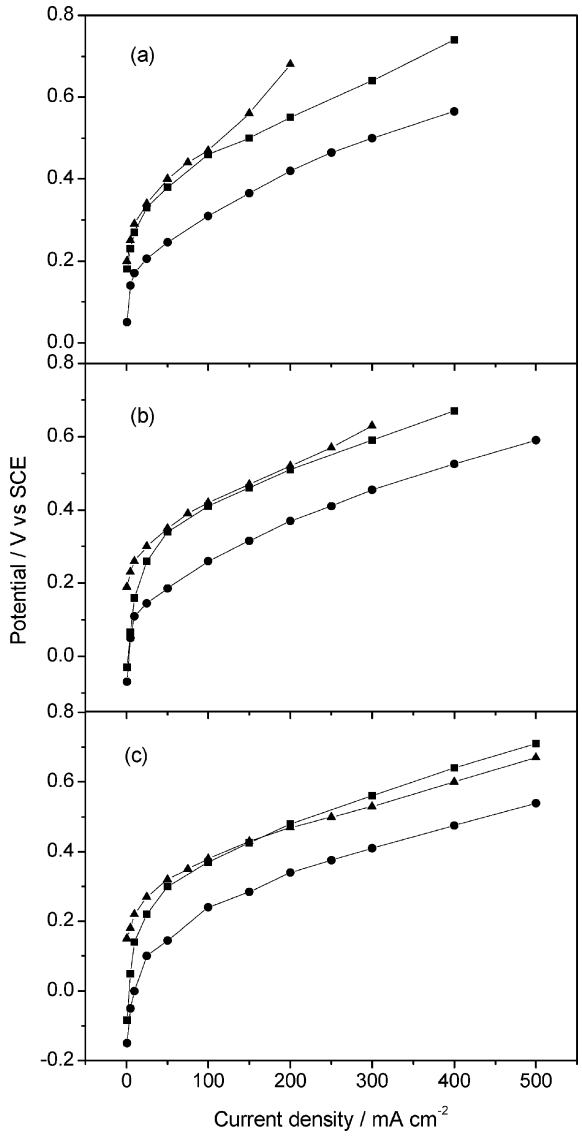

Fig. 5. Nafion® content dependent anode polarization curve for Pt–Ru/MCMB. Methanol concentration 1.0 M; Pt loading 0.3 mg cm^{-2}. Cell temperature: (a) 60, (b) 75 and (c) 90 °C. Key: (■) anode 1, (●) anode 2 and (▲) anode 3.

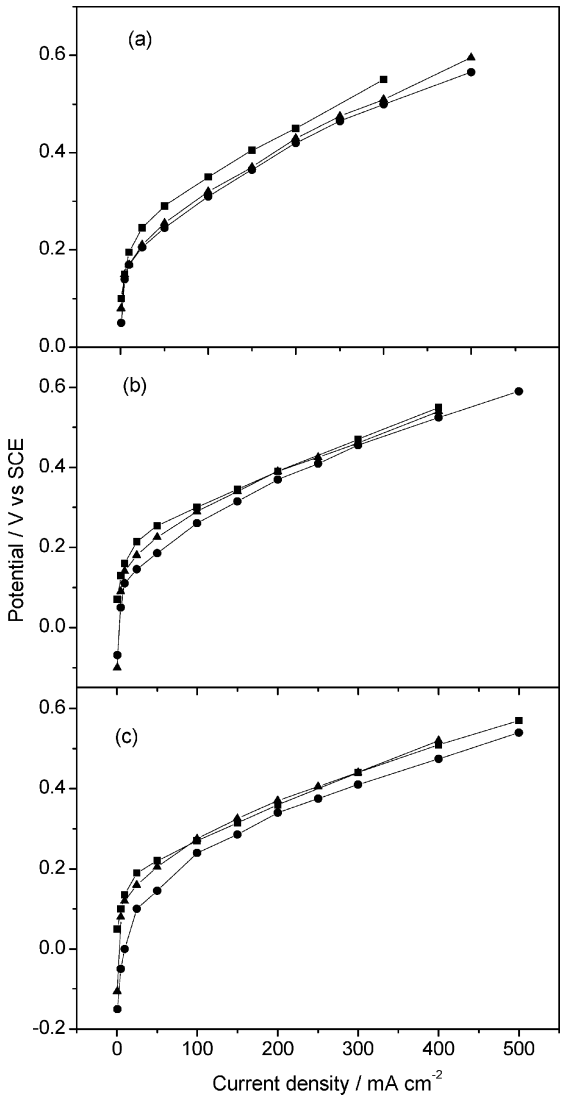

Fig. 6. Pressure of hot press dependent anode polarization curve for anode 2. Methanol concentration 1.0 M; Pt loading 0.3 mg cm^{-2}. Cell temperature: (a) 60, (b) 75 and (c) 90 °C. Key: (■) 5.0, (●) 7.5 and (▲) 10.0 Mpa.

tions of aqueous methanol (0.5–2.0 M) as fuel. When the temperature increases, the overpotential decreases at a rate of 30 mV per 10 °C. The decreased polarization at higher temperature is attributable to a combination of factors consisting of a reduction of cell ohmic resistance, activation polarization and concentration polarization. The result is consistent with the result obtained with the carbon black supported catalysts. It has been reported that, in the range 60 ~ 90 °C, there was an approximate 40 mV drop in the cell potential per 10 °C fall in temperature [27].

Figure 8 shows the concentration dependence of the anode performance at various cell temperatures (anode 2). The polarization of the electrode at the lower methanol concentration (0.5 M) is higher than that at the high methanol concentration, which indicates that there is higher mass polarization at the lower methanol concentration. The anode shows almost the same polarization performance when the methanol concentration is 1.0 and 2.0 M. It was reported that the influence of methanol concentration and liquid flow rate is not critical. A more critical issue is the aspect of methanol conversion in the cell and thus the amount of carbon dioxide produced [27]. Generally, much more attention is focused on the influence of methanol concentration on the total performance of DMFC for the reason of methanol crossover. It has been reported that the selection of methanol concentration, for maximum cell power density, depends on the current density [28].

4. Conclusion

Mesocarbon microbead supported Pt–Ru catalyst exhibits a high catalytic activity for methanol oxidation

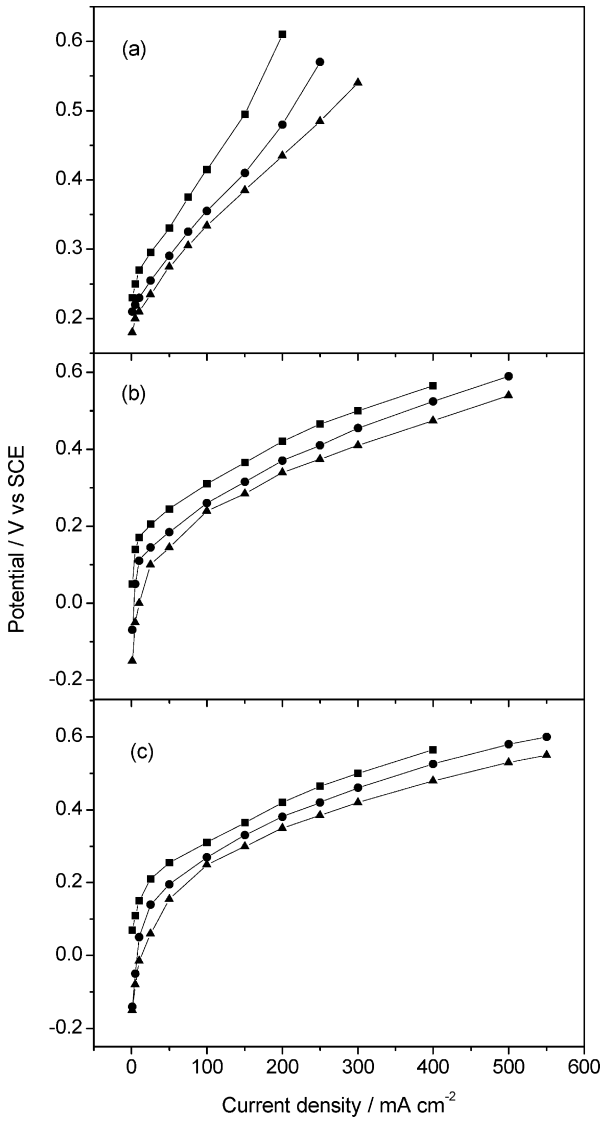

Fig. 7. Temperature dependent anode polarization curve for anode 2. Pt loading 0.3 mg cm^{-2}. Methanol concentration: (a) 0.5, (b) 1.0 and (c) 2.0 M. Key: (■) 60, (●) 75 and (▲) 90 °C.

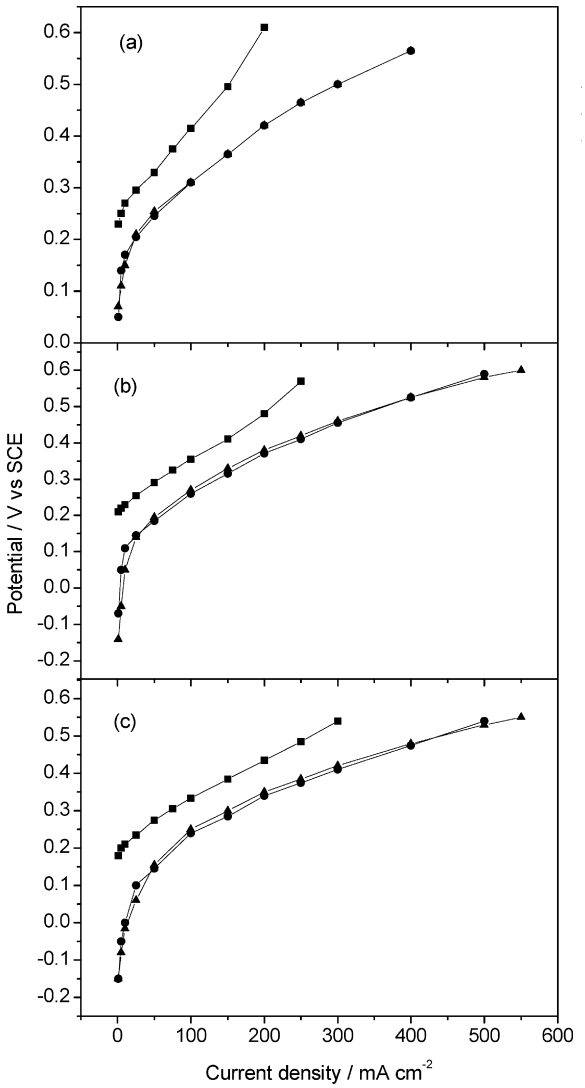

Fig. 8. Concentration dependent anode polarization curve for anode 2. Pt loading 0.3 mg cm^{-2}. Cell temperature: (a) 60, (b) 75 and (c) 90 °C. Key: (■) 0.5, (●) 1.0 and (▲) 2.0 M CH_3OH.

especially at high current density. The Pt–Ru particle size dispersed on the MCMB is larger than that of catalyst prepared with carbon black as support because of the lower specific surface area of the MCMB. The lower anode polarization characteristic at high current density is due to improved mass transport. Further work is ongoing to avoid the form atom of sulfur on the catalyst surface and to reduce the Pt particle size of the supported catalyst and to study the performance of the fuel cell using the MCMB supported catalyst as anode catalyst.

The conditions of preparation of MEAs and the operation of the fuel cell have a great influence on the performance of the supported anode catalysts. The anode with appropriate Nafion® content (10 wt%) and hot press pressure (7.5 MPa) shows the best performance at methanol concentrations >1.0 M at high cell temperature.

References

1. B.D. McNicol, D.A.J. Rand and K.R. Williams, *J. Power Sources* **83** (1999) 15.
2. B.D. McNicol, *Catalyst* **2** (1978) 1243.
3. B.D. McNicol, *J. Electroanal. Chem.* **118** (1981) 71.
4. M. Watanabe, M. Uchida and S. Motoo, *J. Electroanal. Chem.* **199** (1986) 311.
5. H.A. Gasteiger, N. Markovic, P.N. Poss Jr. and E.J. Cairns, *J. Electrochem. Soc.* **141** (1994) 1795.
6. K. Wang, H.A. Gasteiger, N.M. Markovic and P.N. Ross Jr., *Electrochim. Acta* **41** (1996) 2587.
7. S. Surampudi, S.R. Narayanan, E. Vamos, H. Frank, G. Halpert, A. LaConti, J. Kosek, G.K.S. Prakash and G.A. Olah, *J. Power Sources* **47** (1994) 377.
8. N.M. Markovic, H.A. Gasteiger, P.N. Ross Jr., X. Jiang, I. Villegas and M.J. Weaver, *Electrochim. Acta* **40** (1995) 91.
9. A.S. Aricò, P. Creti, E. Modica, G. Monforte, V. Baglio and V. Antonucci, *Electrochim. Acta* **45** (2000) 4319.
10. L. Liu, C. Pu, R. Viswanathan, Q. Fan, R. Liu and E.S. Smotkin, *Electrochim. Acta* **43** (1998) 3657.
11. M. Watanabe, M. Uchida and S. Motoo, *J. Electroanal. Chem.* **229** (1987) 395.

12. M. Hogarth, P. Christensen, A. Hamnett and A. Shukla, *J. Power Sources* **69** (1997) 113.
13. M. Uchida, Y. Aoyama, M. Tanabe, N. Yanagihara, N. Eda and A. Ohia, *J. Electrochem. Soc.* **142** (1995) 2572.
14. U.A. Paulus, U. Endruschat, G.J. Feldmeyer, T.J. Schmidt, H. Bönnemann and R.J. Behm, *J. Catal.* **195** (2000) 383.
15. M. GoÈtz and H. Wendt, *Electrochim. Acta* **43** (1998) 3637.
16. T. Frelink, W. Visscher and J.A.R. Van Veen, *Electrochim. Acta* **39** (1994) 1871.
17. A.K. Shukla, P.A. Christensen, A.J. Dickinson and A. Hamnett, *J. Power Sources* **76** (1998) 54.
18. S. Gamburzev, C. Boyer and A.J. Appleby, *Fuel Cells Bull.* **2** (1999) 6.
19. A. Fischer, J. Jindra and H. Wendt, *J. Appl. Electrochem.* **28** (1998) 277.
20. A.S. Aricò, P. Cretì, H. Kim, R. Mantegna, N. Giordano and V. Antonucci, *J. Electrochem. Soc.* **143** (1996) 3950.
21. K. Kinoshita and P. Stonehart, 'Modern Aspects of Electrochemistry' (Plenum, New York, 1977).
22. M. Watanabe, H. Sei and P. Stonehart, *J. Electroanal. Chem.* **261** (1989) 375.
23. M. Watanabe, S. Saegusa and P. Stonehart, *Chem. Lett.* **9** (1989) 1487.
24. C. Boyer, S. Gamburzev, O. Velev, S. Srinivasan and A.J. Appleby, *Electrochim. Acta* **43** (1998) 3703.
25. M. Uchida, Y. Fukuoka, Y. Sugawara, N. Eda and A. Ohta, *J. Electrochem. Soc.* **143** (1996) 2245.
26. M. Uchida, Y. Aoyama, N. Eda and A. Ohta, *J. Electrochem. Soc.* **142** (1995) 4143.
27. K. Scott, W.M. Taama and P. Argyropoulos, *J. Appl. Electrochem.* **28** (1998) 1389.
28. K. Scott, W.M. Taama, P. Argyropoulos and K. Sundmacher, *J. Power Sources* **83** (1999) 204.